Species-specific isotope tracking of mercury uptake and transformations by pico-nanoplankton in an eutrophic lake

Thibaut Cossart, Javier Garcia-Calleja, Isabelle A.M. Worms, Emmanuel Tessier, Killian Kavanagh, Zoyne Pedrero, David Amouroux, Vera Slaveykova

Environmental Pollution 288 (2021) 117771

Contents lists available at ScienceDirect

Environmental Pollution

journal homepage: www.elsevier.com/locate/envpol

Species-specific isotope tracking of mercury uptake and transformations by pico-nanoplankton in an eutrophic lake☆

Thibaut Cossart [a], Javier Garcia-Calleja [b], Isabelle A.M. Worms [a], Emmanuel Tessier [b], Killian Kavanagh [a], Zoyne Pedrero [b], David Amouroux [b], Vera I. Slaveykova [a,*]

[a] Environmental Biogeochemistry and Ecotoxicology, Department F.-A. Forel for Environmental and Aquatic Sciences, Earth and Environmental Sciences, Faculty of Sciences, University of Geneva, Uni Carl Vogt, Bvd Carl-Vogt 66, CH-1211, Geneva 4, Switzerland

[b] Université de Pau et des Pays de l'Adour, E2S UPPA, CNRS, IPREM, Institut des Sciences Analytiques et de Physico-chimie pour l'Environnement et les matériaux, Pau, France

ARTICLE INFO

Keywords:
Natural pico-nanoplankton
Inorganic mercury
Methylmercury
Enriched stable isotopes
Eutrophic lake
Biotic transformations

ABSTRACT

The present study aims to explore the bioaccumulation and biotic transformations of inorganic (iHg) and monomethyl mercury (MMHg) by natural pico-nanoplankton community from eutrophic lake Soppen, Switzerland. Pico-nanoplankton encompass mainly bacterioplankton, mycoplankton and phytoplankton groups with size between 0.2 and 20 μm. Species-specific enriched isotope mixture of ^{199}iHg and ^{201}MMHg was used to explore the accumulation, the subcellular distribution and transformations occurring in natural pico-nanoplankton sampled at 2 different depths (6.6 m and 8.3 m). Cyanobacteria, diatoms, cryptophyta, green algae and heterotrophic microorganisms were identified as the major groups of pico-nanoplankton with diatoms prevailing at deeper samples. Results showed that pico-nanoplankton accumulated both iHg and MMHg preferentially in the cell membrane/organelles, despite observed losses. The ratios between the iHg and MMHg concentrations measured in the membrane/organelles and cytosol were comparable for iHg and MMHg. Pico-nanoplankton demethylate added ^{201}MMHg (~4 and 12% per day depending on cellular compartment), although the involved pathways are to further explore. Comparison of the concentrations of ^{201}iHg formed from ^{201}MMHg demethylation in whole system, medium and whole cells showed that 82% of the demethylation was biologically mediated by pico-nanoplankton. No significant methylation of iHg by pico-nanoplankton was observed. The accumulation of iHg and MMHg and the percentage of demethylated MMHg correlated positively with the relative abundance of diatoms and heterotrophic microorganisms in the pico-nanoplankton, the concentrations of TN, Mg^{2+}, NO_3^-, NO_2^-, NH_4^+ and negatively with the concentrations of DOC, K^+, Na^+, Ca^{2+}, SO_4^{2-}. Taken together the results of the present field study confirm the role of pico-nanoplankton in Hg bioaccumulation and demethylation, however further research is needed to better understand the underlying mechanisms and interconnection between heterotrophic and autotrophic microorganisms.

1. Introduction

Mercury (Hg) is naturally present in the Earth crust, however human activities have significantly disturbed its natural biogeochemical cycle (Driscoll et al., 2013; Eagles-Smith et al., 2016). Consequently, the concentrations of mercury compounds in the aquatic environment have significantly increased (Streets et al., 2017). In aquatic environment mercury speciation is dominated by inorganic (iHg) and monomethyl mercury (CH_3Hg^+, MMHg), but their relative abundance depends on key transformations, such as reduction/oxidation and methylation/demethylation (Branfireun et al., 2020; Dranguet et al., 2014; Le Faucheur et al., 2014). These transformations processes, and thus Hg speciation, can be influenced by various abiotic factors, such as light radiations (Deng et al., 2009; Deng et al., 2008; Du et al., 2019; Monperrus et al., 2007), organic matter (Bravo et al., 2017; Lavoie et al., 2019; Lee and Fisher, 2017), pH (Boullemant et al., 2009; Kelly et al., 2003; Le Faucheur et al., 2011), micro- and macronutrients (Driscoll et al., 2012; Kim et al., 2014; Van et al., 2016) and, by biotic factors,

☆ This paper has been recommended for acceptance by Sarah Harmon.

* Corresponding author.
E-mail address: vera.slaveykova@unige.ch (V.I. Slaveykova).

https://doi.org/10.1016/j.envpol.2021.117771
Received 4 March 2021; Received in revised form 6 July 2021; Accepted 8 July 2021
Available online 9 July 2021

such as the microbial community activity (Bravo and Cosio, 2020; Du et al., 2019). Therefore, the understanding of the Hg transformations is a key for assessing the impact of Hg in the aquatic environment, given different reactivity of Hg species to biota, their bioaccumulation and biomagnification potential (Branfireun et al., 2020; Gregoire and Poulain, 2014; Hsu-Kim et al., 2013; Le Faucheur et al., 2014).

In this study, we focus on mercury bioaccumulation and biotransformation by natural pico-nanoplankton. Pico-nanoplankton comprise primarily bacterioplankton, mycoplankton and phytoplankton with size between 0.2 and 20 μm (Sieburth et al., 1978). Up to now, a significant attention has been paid on Hg transformation in anoxic aquatic environment by the heterotrophic bacteria and other methanogens (Bratkic et al., 2018; Du et al., 2019; Hsu-Kim et al., 2013; Lin, 2011; Pedrero et al., 2012). The role of phytoplankton in both abiotic and biotic transformations of Hg is understudied. The limited literature revealed that phytoplankton could affect Hg speciation directly by accumulation (Lanza et al., 2017; Lee and Fisher, 2016; Pickhardt and Fisher, 2007) and subsequent biotic (Bravo et al., 2014; Wu and Wang, 2014) and abiotic transformations (Kritee et al., 2018), and/or indirectly via the production of biogenic ligands with the potential to alter Hg speciation and thus its bioavailability (Chen et al., 2014; Gregoire and Poulain, 2014; Wang et al., 2011). Laboratory studies have demonstrated the ability of cyanobacterium *Synechococcus leopoldiensis*, green alga *Chlorella autotrophica*, dinoflagellate *Isochrysis galbana* and diatom *Thalassiosira weissflogii* to reduce iHg into dissolved gaseous mercury (DGM, Hg^0) (Lefebvre et al., 2007; Wu and Wang, 2014). Photoreduction of iHg to DGM was significantly accelerated by the presence of green alga *Chlorella vulgaris* or cyanobacteria *Anabaena cylindrica* (Deng et al., 2009; Deng et al., 2008). It is rather rare to find studies showing the capacity of phytoplankton to methylate iHg (Gregoire and Poulain, 2014; Sigel et al., 2015). For example, cyanobacterium *Nostoc poludosum* produced MMHg, however it represented only 0.0023% of the THg in the cyanobacterium biomass (Franco et al., 2018). In addition, green alga *Chlamydomonas reinhardtii* was shown to demethylate MMHg (Bravo et al., 2014). Some cyanobacteria and green algae produced cinnabar (α-HgS) and *meta*-cinnabar (β-HgS), a process catalysed by intracellular thiols (R–SH), such as glutathione, phytochelatins and/or metallothionein (Gregoire and Poulain, 2014; Kelly et al., 2006). These transformations were species-specific with highest transformation rates observed for green algae and the lowest for diatoms (Wu and Wang, 2014). Phytoplankton species also excrete biogenic ligands, such as thiols, which were shown to alter Hg speciation, bioaccumulation and transformations (Skrobonja et al., 2019).

Pico-nanoplankton are at the base of the aquatic food webs and serve as an entry point of Hg species into organisms of higher tropic levels (Lee and Fisher, 2016; Wu et al., 2020). Since the biotic transformations by microorganisms are presumably intracellular and because the assimilation efficiency of Hg in the food webs is higher when Hg is accumulated in cytosol, both the concentration and subcellular distribution of Hg species should be considered to predict its potential for transfer through the trophic webs.

In such a context, the present study aims to get insight into the role of natural pico-nanoplankton community in biotic transformations of two mercury species prevailing in the aquatic environment: iHg and MMHg. To this end, pico-nanoplankton were sampled at two different depths in the eutrophic lake Soppen (Switzerland) and spiked with a mixture of enriched stable isotopes of ^{199}iHg and ^{201}MMHg. The uptake, the subcellular distribution and the biotic methylation and demethylation were assessed, together with the composition of the pico-nanoplankton, and major water quality variables.

2. Material and methods

2.1. Study site description

The lake Soppen is located in Buttisholtz (Canton of Lucerne, Switzerland, Fig. S1), at an elevation of 596 m. It has a surface area of 0.227 km^2 with a maximal and mean depths of 26 and 12.3 m, respectively (Langenegger et al., 2019). Most of the year the lake is stratified with a thermocline around 5 and 10 m depth (Fig. S2) with anoxic bottom water (Gruber et al., 2000; Vachon et al., 2019). This anoxic conditions persist below 7 m most of the year (during 9–10 months) with a mixing period of water occurring at the beginning of the year (Gruber et al., 2000). The lake is eutrophic given the intense agriculture activities in its watershed. The total phosphorus content of the water column has been determined at 40 mg L^{-1} (Vachon et al., 2019). This lake is used as a model system for research in sedimentology and for exploring the biological dynamic of higher trophic levels (Gruber et al., 2000; Lotter, 2001), but no information is available for planktonic microorganisms and their turnovers.

2.2. Determination of water physicochemical parameters and pico-nanoplankton community composition

CTD probe (CTD90M, Sea&Sun Technology, Germany) was used for in-situ measurements of pH, conductivity and temperature. Dissolved organic carbon (DOC) and total nitrogen (TN) concentrations were determined by Shimadzu TOC-L series analyser (TOC-5000A, Shimadzu, Japan). Major cations and anions were separated (cations: IC Dionex IonPac CS12 and, anions: IC Dionex IonPac AS19) and measured by ion exchange chromatography (Dionex ICS-3000, ThermoFisher Scientific Inc., USA).

The chlorophyll depth profiles of different algal groups were obtained by fluoroprobe (FluoroProbe, bbe Moldaenke GmbH, Germany), and used to assess phytoplankton composition including "blue green algae" (cyanobacteria), "green algae", "diatoms" and "cryptophyta" based on the fluorescence emission spectrum of the chlorophyll *a* of each class (Garrido et al., 2019; Schutte et al., 2020). The sampling depths were determined to obtain the maximum of biomass and different composition of phytoplankton communities. Quantification of heterotrophic microorganisms has been done by flow cytometry (Accuri C6, BD Biosciences, USA) following staining with SYBR green (Sybr green I nucleic acid gel stain, 10000x in DMSO, ThermoFisher Scientific Inc., USA) after fixation of samples with glutaraldehyde at a final concentration of 0.25% (grade II, 25% in H_2O, Sigma-Aldrich, USA) (Coclet et al., 2019; Delpy et al., 2018).

2.3. Exposure of pico-nanoplankton to a mixture of ^{199}iHg and ^{201}MMHg

Exposure has been performed in lake water enriched with pico-nanoplankton under well controlled laboratory conditions. To this end, 20 L of water were sampled at two depths of interest (6.6 m and 8.3 m) with pre-cleaned Niskin bottles. All the materials for field and laboratory work (e.g. bottles, syringes, vials, tips) were acid pre-cleaned using several baths, i.e. 10% HNO_3 (pro-analysis, Merck, Darmstadt, Germany), and 10% HCl (pro-analysis, Merck, Darmstadt, Germany) during 1 h under sonication (Branson Ultrasonic cleaner 5510, Emerson Electric Co., USA), then rinsed with ultrapure water (Milli-Q Direct 8, Merck, Germany) and left to dry under laminar flow hood. Next, the materials were autoclaved at 121 °C during 30 min with 1 bar pressure (LVSA 50/70, Zirbus Technology, Benelux). Further details can be found in a previous work (Dranguet et al., 2017).

The cell density was artificially increased by a factor of 7.3 (from 1.5 × 10^5 to 1.1 × 10^6 cells mL^{-1} for depth 1 and, from 3.9 × 10^5 to 2.8 × 10^6 cells mL^{-1} for depth 2). To this end, cells were preconcentrated by centrifugation and resuspended in lake water filtered on 0.22 μm GPWP filters (hydrophilic polyethersulfone) (Fig. S3). According to the experimental design and the planktonic classification based on cellular size (Sieburth et al., 1978), harvested planktonic microorganisms were composed of pico- and nanoplankton with a size between 0.2 and 20 μm, which comprised mainly bacterioplankton, mycoplankton and phytoplankton. Six sub-samples of 110 mL were further treated. Three of them

were spiked with a mixture of Hg enriched stable isotopes containing 1 × 10^{-9} mol L^{-1} of inorganic ^{199}iHg (ISC Science, Spain, ^{199}iHg in HCl 2%, isotopic relative abundance: 91.4%) and 1 × 10^{-10} mol L^{-1} of ^{201}MMHg (^{201}MMHg, ISC Science, Spain, $^{201}CH_3Hg^+$ in 3:1 acetic acid/methanol solution, isotopic relative abundance: 96.5%). The other three sub-samples were used as unexposed biotic control. Exposures were performed for 24 h and mimic natural diurnal cycle. At the end, 10 mL from exposure and from unexposed biotic control were sampled and acidified with 4.2 mL of supra pure nitric acid (65%, HNO_3) to reach a final HNO_3 concentration about 5 N for the determination of the total Hg concentration in the system (whole system, Fig. S3).

2.4. Bioaccumulation and transformation of Hg species by pico-nanoplankton

The bioaccumulation and transformation of iHg and MMHg by whole pico-nanoplankton cells, membrane/organelles and cytosol fractions were determined, as well as total and dissolved iHg, and MMHg concentrations in the system (see workflow on supplementary Fig. S3). At the end of the 24 h-exposure, pico-nanoplankton were separated from the medium by gentle centrifugation (4330×*g*, 25 min). Supernatant was collected, acidified with HCl (supra pure, 30%) to a final concentration of 1% and used to determine the concentration of dissolved ^{199}iHg and ^{201}MMHg. The pellet containing pico-nanoplankton was rinsed with 0.22 μm filtered lake water, acidified with 1 mL of HNO_3 (supra pure, 65%) and digested to determine whole cell Hg concentration and evaluate uptake and biotic transformations. To get further insight into which biological compartment the Hg predominantly accumulates and possibly transforms, half of the pico-nanoplankton suspension were centrifuged, washed with filtered lake water, and then centrifuged again. To separate membranes and organelles from cytosol fraction, the pellet was placed in 2 mL Eppendorf and flash-frozen in liquid nitrogen. To break cells, 0.5 mL of 50% methanol solution (v/v in milliQ water) were added with glass beads, then vortexed 6 × 15 s and placed on ice between fractionations. Then, samples were centrifuged during 6 min at 12052×*g* (Centrifuge 541R, Eppendorf, Germany). Obtained pellets (membrane/organelles fraction) and supernatant (cytosol) were separated, acidified and stored at +4 °C before analysis.

2.5. Mercury compounds isotopic dilution analysis by gas chromatography coupled to inductively plasma mass spectrometry

The Hg analysis was carried out by gas chromatography coupled to inductively plasma mass spectrometry (GC–ICP–MS) and the quantification of Hg species was achieved by isotopic dilution analysis (Rodriguez-Gonzalez et al., 2013). All measurement required a derivatization step in order to produce volatile ethylated Hg species allowing its separation by gas chromatography (Monperrus et al., 2008; Rodriguez-Gonzalez et al., 2013). After a microwave digestion for pico-nanoplankton pellets (4 min, 75 °C, Discover and Explorer SP-D 80 system, CEM, NC USA), samples were transferred in 22 mL glass vial containing 5 mL of acetate buffer (acetic acid/acetate, 0.1 M, pH = 3.9). The quantification of spiked Hg isotopes (^{199}iHg and ^{201}MMHg present in all studied samples) is made possible by adding to the samples an appropriate concentration of a second set of isotopes (^{198}iHg and ^{202}MMHg) as internal calibration standards (Bouchet et al., 2018). After equilibration, pH was adjusted between 3.85 and 4.05. Then, 250 μL of GC organic solvent (Isooctane: 2,2,4 trimethylpentane, C_8H_{18}) and 80 μL of derivatizing agent, tetraethylborate ($NaBEt_4$, 5% v/v, Merseburger spezial Chemikalien, Germany) were added and samples were shaken during 20 min on elliptic table. At the end, the organic phase containing Hg species was recovered in vial for GC–ICP–MS analysis. Determination of total mercury species concentration was done on a Thermo Scientific GC-ICP-MS (Bouchet et al., 2018; Rodriguez-Gonzalez et al., 2013). The detection limit of Hg compounds for GC-ICP-MS analytical method were 4.72 × 10^{-13} mol L^{-1} and 7.70 × 10^{-14} mol L^{-1} for iHg and MMHg, respectively. These values allowed to estimate the minimum detectable concentration of newly formed Hg species after transformation: ^{201}iHg = (7.48 ± 3.50) × 10^{-12} mol L^{-1} and ^{199}MMHg = (4.58 ± 2.73) × 10^{-12} mol L^{-1}. The natural Hg background in the lake water have been also determined. Details about the mathematical approach used for the quantification of endogenous (natural) and exogenous (enriched) Hg isotope species (iHg and MMHg) concentrations by double-double species-specific isotope dilution analysis based on isotopic pattern deconvolution (IPD) can be found in our previous studies (Bouchet et al., 2018; Rodriguez-Gonzalez et al., 2013) and supplementary information (SI).

2.6. Assessment of potential biotic transformations

The change in the ratio between the difference of transformed Hg species (^{199}MMHg and ^{201}iHg) concentrations before and after exposure and, the spiked isotopes concentrations (^{199}iHg and ^{201}MMHg) before exposure in the whole-cell and the subcellular fractions were used to estimate the percentage of potentially methylated (Eq. (1)) and demethylated (Eq. (2)) mercury species (Bridou et al., 2011).

$$\%\ Hg, meth = \frac{[^{199}MMHg]_{t24} - [^{199}MMHg]_{t0}}{[^{199}iHg]_{t0}} \times 100 \quad (1)$$

$$\%\ Hg,\ demeth = \frac{[^{201}iHg]_{t24} - [^{201}iHg]_{t0}}{[^{201}MMHg]_{t0}} \times 100 \quad (2)$$

2.7. Statistical analysis

One-way Analysis of Variance (ANOVA) followed by All Pairwise Multiple Comparison by Student-Newman-Keuls method (p-value < 0.05) was performed to determine significant differences between data. Further statistical analysis were performed to explore possible correlations between Hg accumulation and transformations with both physicochemical and biological variables, using R-Studio with FactoMineR (Husson et al., 2008), Vegan (Crist et al., 2003) and Corrplot (Friendly, 2002) packages. Correlation matrices were built on the base of Pearson correlation coefficients (PCC) between each parameter. These analyses allowed to determine the influence of physicochemical variables and pico-nanoplankton community composition on Hg uptake and transformations. Dependency of each variables found in correlation matrices was compared with the distance between each of them by redundancy analysis (RDA, SI).

3. Results and discussion

3.1. Lake water quality variables at the sampling location and Hg background concentrations in water

Conductivity was 250 μS cm^{-1} at 6.6 m and 300 μS cm^{-1} at 8.3 m, and temperature was 18 °C and 10 °C for each depth (Table S1). These values agreed with the previous measurements in lake Soppen for a similar sampling period (Lotter, 2001; Tang et al., 2018). Dissolved oxygen concentration decreased with the depth (Fig. S2C). This decrease could be linked with the increase of biomass (Fig. 1A) and probably with a higher heterotrophic activity. A thermocline and an oxycline were between 6 and 10 m during sampling period. The TN concentrations at both depths (>2.5 mg L^{-1}) were higher than the values measured in the lake in the past (Lotter, 2001) or in other eutrophic lakes (Wang et al., 2019) and approached those found in hypereutrophic lakes (Wang et al., 2012c). The DOC values were 7.4 mg L^{-1} for 6.6 m and about 6.5 mg L^{-1} for 8.3 m depth, quite high and consistent with values typically found in eutrophic lakes. No significant difference was found between the concentrations of the cations for water sampled from two depths, whereas the concentrations of the analysed anions were significantly different (Table S1). Overall, the high nutrient concentrations are consistent with

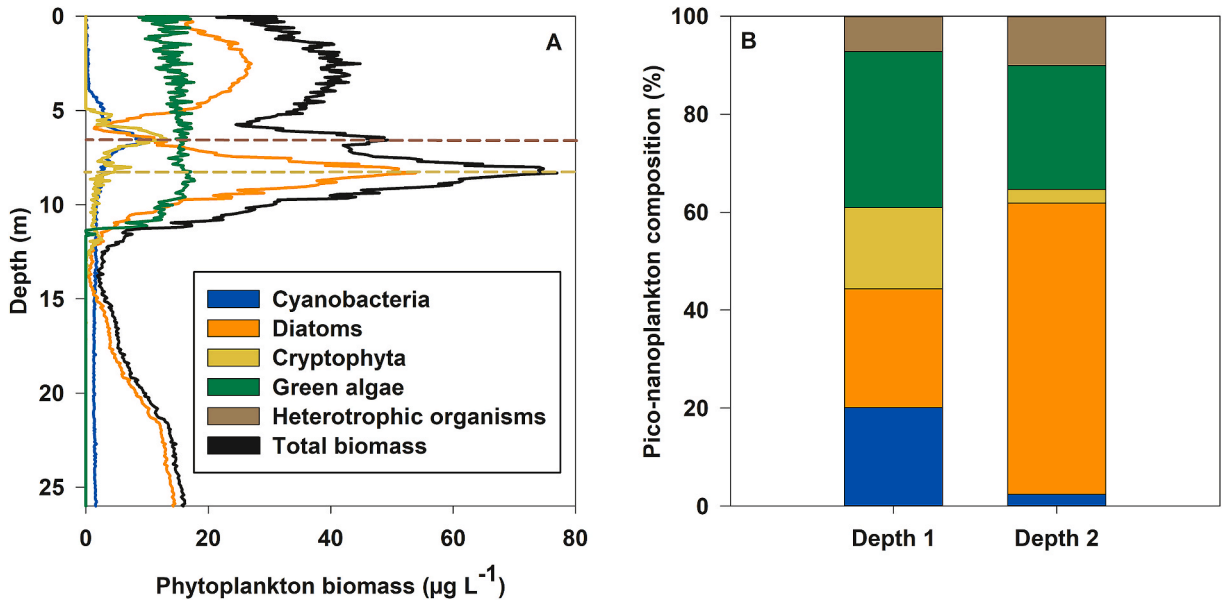

Fig. 1. Pico-nanoplankton groups. (A) biomass and chlorophyll *a* profiles of phytoplankton (µg L^{-1} of pigment) determined in-situ with FluoroProbe; (B) proportion of bacterioplankton + mycoplankton and different phytoplankton groups expressed in percentages in the total biomass. The abundance of heterotrophic microorganisms was determined by flow cytometry following SYBR green staining. Dash lines represent two depths chosen for sampling 6.6 and 8.3 m. (For interpretation of the references to colour in this figure legend, the reader is referred to the Web version of this article.)

the eutrophic state of lake Soppen. The natural background concentrations in the filtered lake water were (3.79 ± 1.77) × 10^{-11} mol L^{-1} for iHg and (5.98 ± 3.59) × 10^{-12} mol L^{-1} for MMHg, concentrations about 26 and 17 times lower than the added spikes enriched in ^{199}iHg and ^{201}MMHg isotopes.

Natural iHg and MMHg concentrations are within the range of the total Hg (THg, 2.1 × 10^{-11} – 2.3 × 10^{-10} mol L^{-1}) and MMHg (2.0 × 10^{-13} – 1.2 × 10^{-12} mol L^{-1}) measured in the filtered water from other shallow eutrophics lakes in China (Chen et al., 2021; Wang et al., 2012a; Wang et al., 2012b). However, the background concentrations found in lake Soppen were higher than those reported for eutrophic reservoir Tianmu, China (Razavi et al., 2015)) or many of the world's great lakes (Chen et al., 2021; Guédron et al., 2017). MMHg represented 10.6% of the THg concentration, which is higher than the percentages found in lake Taihu (0.12–3.5%) (Wang et al., 2012a), Dianchi (0.22–1.50%) (Wang et al., 2012b) or reservoir Tianmu (2.0%) (Razavi et al., 2015). Such high percentage of MMHg could be probably related with the increase in organic matter production and remineralization typical for eutrophication (Guédron et al., 2017; Soerensen et al., 2016). It could stimulate microbial Hg methylation resulting in an increase of MMHg in water of shallow lakes where the reemission from lake sediments could be high (Yang et al., 2020).

3.2. Characterization of pico-nanoplankton composition

Vertical profiles of the chlorophyll *a* informing about the total biomass (Fig. 1A) showed two peaks corresponding to 6.6 m (49.3 µg L^{-1}) and 8.3 m (76.9 µg L^{-1}), inside the thermocline of the lake (Fig. S2B). The first peak corresponded to an increased abundance of cyanobacteria (9.5 µg L^{-1}) and cryptophyta (13.1 µg L^{-1}) and, the second one to diatoms (53.8 µg L^{-1}).

The abundance of green algae in the deeper sample was also high (~16.8 µg L^{-1}, Fig. 1A). The total biomass and the proportion between different phytoplankton groups (Fig. 1B), i.e. cyanobacteria and diatoms, suggest that the lake was mesotrophic/eutrophic during the sampling period (early autumn) (Chen et al., 2008; Poste et al., 2015; Wetzel, 2001; Yu et al., 2020). The obtained chlorophyll *a* profiles at the sampling period could be also explained by a recent phytoplankton bloom event in the lake Soppen. The abundance of green algae remained constant from the water surface until the end of the thermocline (~14.6 ± 2 µg L^{-1}) then quickly dropped (Fig. 1A). The biomass of diatoms was close to the one of green algae at the water surface (~16.7 ± 2 µg L^{-1}) but reached a first peak around 2.5 m depth (27.1 µg L^{-1}) and fell to a minimal value around 6 m depth (1.4 µg L^{-1}).

A second peak for diatoms was observed at 8.3 m with a maximum of 53.89 µg L^{-1}. The abundance of diatoms then decreased significantly around 14 m depth and increased again (~14.4 µg L^{-1}) (Fig. 1A). This increase could be related to the presence of a deep chlorophyll maximum (DCM) (Leach et al., 2018). Several studies have shown that DCM is usually dominated by diatoms (Hamilton et al., 2010; Leach et al., 2018; Simmonds et al., 2015). In addition, quite high bacterial density was found in the DCM in comparison with the water column (Leach et al., 2018). Indeed, the abundance of heterotrophic picoplankton was found higher at depth 2 than at depth 1 (Fig. 1B). This is consistent with dissolved oxygen profile (Fig. S2) and suggests that the heterotrophic activity is to considered when exploring Hg transformations. Cyanobacteria and cryptophyta followed almost the same trend as diatoms throughout the depth profile. They were absent in the shallowest water whereas below 5 m, their abundance quickly increased to reach a maximum at 6.6 m corresponding to 9.48 µg L^{-1} for cyanobacteria and 13.16 µg L^{-1} for cryptophyta. The abundances of cyanobacteria and cryptophyta then slowly decreased reaching a background value of 1.47 µg L^{-1} at 10 m depth and beyond for cyanobacteria while no cryptophyta were detected below 13.7 m depth (Fig. 1A).

The proportions of different groups of pico- and nanoplankton at the two sampling depths diverged (Fig. 1B). The community at 6.6 m was composed by 20% of cyanobacteria, 25% of diatoms, 17% of cryptophyta, 31% of green algae and 7% of heterotrophic microorganisms. The community at 8.3 m was dominated by diatoms (~60% of the community) and contained 2% of cyanobacteria, 3% of cryptophyta, 25% of green alga and 10% of heterotrophic microorganisms. Diversity index, H′ considering both the abundance and evenness, was higher for the community in shallower sample (H' = 2.2 at depth 1 *versus* H' = 1.5 at depth 2) and, evenness index, J' was lower for the community at depth 2 (J' = 0.95 at depth 1 and, J' = 0.67 at depth 2).

3.3. Bioaccumulation and subcellular distribution of iHg and MMHg

Pico-nanoplankton communities sampled in the lake Soppen accumulated a significant amount of both Hg species: $(3.5 \pm 0.3) \times 10^{-19}$ mol cell^{-1} and $(3.7 \pm 0.2) \times 10^{-19}$ mol cell^{-1} of ^{199}iHg and, $(2.3 \pm 0.8) \times 10^{-20}$ mol cell^{-1} and $(3.1 \pm 0.1) \times 10^{-20}$ mol cell^{-1} of ^{201}MMHg for depth 1 and depth 2, respectively (Fig. S4). The concentrations of the ^{199}iHg accumulated by pico-nanoplankton were about 10 times higher than that of ^{201}MMHg in agreement with the their exposure concentrations and despite the Hg losses measured in the system.

Comparison of the concentrations of iHg and MMHg in the whole system (lake water + pico-nanoplankton) and the sum of the dissolved and whole cell iHg and MMHg showed an existence of losses over 24h period corresponding to about 45% for iHg and 38% for MMHg (Fig. S4). These losses could be due to a volatilization of Hg^0 following the biotic and abiotic transformations in the system or adsorption to the glassware. Additional leaching experiments with HNO_3 on the empty containers at the end of exposure, revealed that the amount of the adsorbed Hg to the glassware corresponded to less than 10% of the amount of Hg added in the exposure medium. Thus, it seems more plausible that biotic and abiotic transformations or other unknow processes contribute to these losses.

Uptake of ^{199}iHg was similar for the pico-nanoplankton sampled at depth 1 and 2, whereas ^{201}MMHg uptake was significantly higher in the community at depth 2 (Fig. 2A). The concentrations of both Hg species were higher in the community dominated by diatoms sampled at depth 2. This observation could be related with differences in the cell wall composition of the different groups of pico-nanoplankton, e.g. silica frustule of diatoms is known to influence trace metal – cell interactions (Ellwood and Hunter, 2000; Jaccard et al., 2009; Mu et al., 2017). For both ^{199}iHg and ^{201}MMHg accumulated preferentially in the membrane/organelle fractions. Indeed, the concentrations of iHg and MMHg in the membrane/organelle fraction were 7 and 2 times higher than those determined in the cytosolic fraction (Fig. 2B). Even not predominant (relative abundance 7%–10%), heterotrophic microorganisms could also play an important role in the accumulation of Hg by the pico-nanoplankton (Gregoire and Poulain, 2014). However, the composition of bacterio- and mycoplankton need also to be better characterized to be able to decipher their role in Hg fate in eutrophic lakes dominated by autotrophs (Fig. 1).

The ratios of Hg concentrations determined in membrane/organelles and cytosol fractions were comparable for ^{199}iHg and ^{201}MMHg (Fig. S5). This observation is somehow opposite to the previous findings obtained from axenic cultures of green alga *C. reinhardtii* showing that MMHg accumulated predominantly in cytosolic fraction (2 h exposure to several Hg concentrations: 10^{-11} – 10^{-8} mol L^{-1} iHg and 10^{-11} – 10^{-9} mol L^{-1} MMHg) (Beauvais-Fluck et al., 2017), whereas for the same alga iHg prevailed in membrane fraction (5×10^{-7} mol L^{-1} iHg compared with 3.5×10^{-9} mol L^{-1} MMHg after 72 h exposure) (Le Faucheur et al., 2014; Wu and Wang, 2011). However, the concentration of MMHg in the cellular membranes of other green alga *Selenastrum capricornutum* was much higher than the one in the cytosol fraction (Skrobonja et al., 2019). X-ray fluorescence mapping also revealed that Hg species were more concentrated in the cell-wall of diatoms ([THg] = 5×10^{-9} mol L^{-1}, mixture of several diatoms sampled in Oak Ridge, Tennessee) (Gu et al., 2014). Another study on marine diatom *T. weissflogii* revealed that Hg species mainly accumulated in cytosol and more specifically in metallothionein-like proteins (MTLP) (Wu and Wang, 2013), but in this case the Hg concentrations and the speciation, exposure duration as well as experimental procedure for the distinction between cytosolic (i.e. intracellular) and adsorbed Hg contents were very different to enable direct comparison with our findings. In addition, the distinction between cytosolic and membrane/organelles fractions is operational and subject to high uncertainty. Nevertheless, the knowledge of the subcellular distribution of iHg and MMHg is central for better understanding of mercury trophic transfer and toxicity outcome (Le Faucheur et al., 2014).

Statistical analysis that the accumulation of iHg in both subcellular fractions was positively correlated with TN, Mg^{2+}, NO_3^-, NO_2^-, NH_4^+ concentrations and negatively correlated with the concentrations of DOC, K^+, Na^+, Ca^{2+}; SO_4^{2-} (Fig. 3A). The formation of complexes between the dissolved organic matter (DOM) and iHg is known to reduce the uptake by various algae and bacteria (Branfireun et al., 2020; French et al., 2014). Therefore the negative correlation between the iHg accumulation by pico-nanoplankton dominated by phototrophs is plausible. However, ^{201}MMHg accumulation in membrane/organelles fraction were positively correlated with concentrations of K^+, Na^+, Ca^{2+}, SO_4^{2-} and DOC. Such positive correlation between the MMHg accumulation and the DOC could be expected given the role of fresh humic and algal derived organic matter in the increase of the MMHg concentrations in surface waters (Herrero Ortega et al., 2018). The above observations are in general agreement with the current understanding that metal

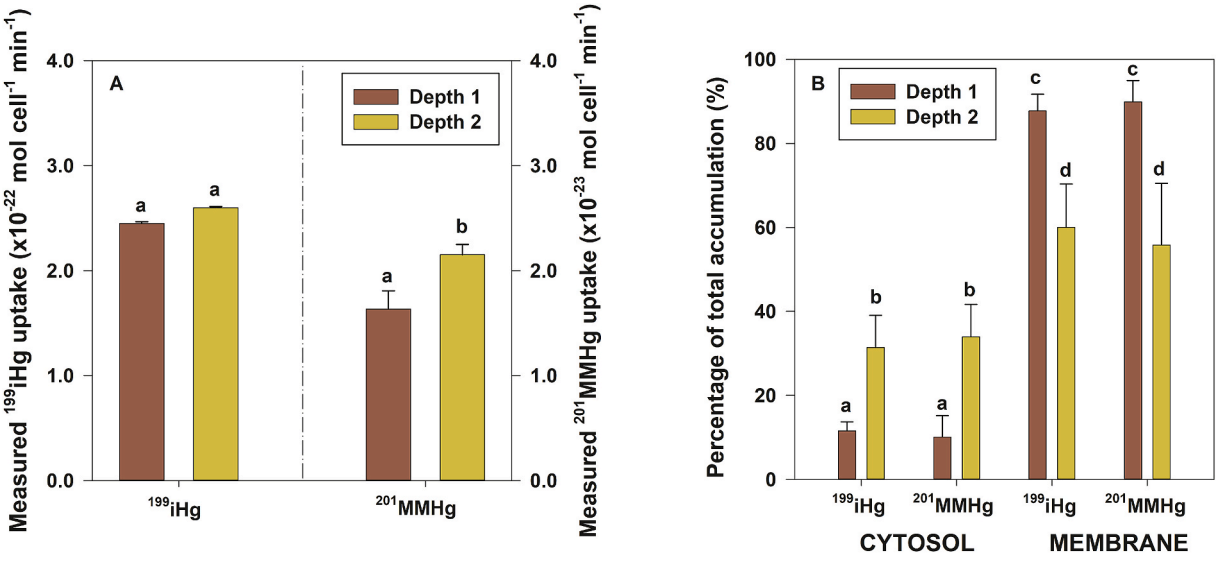

Fig. 2. Accumulation of ^{199}iHg and ^{201}MMHg in pico-nanoplankton. (A) whole cell accumulation, (B) subcellular distribution of Hg species in the subcellular fractions versus Hg in whole cell. The values are average ± standard deviation for triplicate experiments (n = 3). Letters indicate statistically significant difference between treatments (Student-Newman-Keuls test, *p*-value < 0.05).

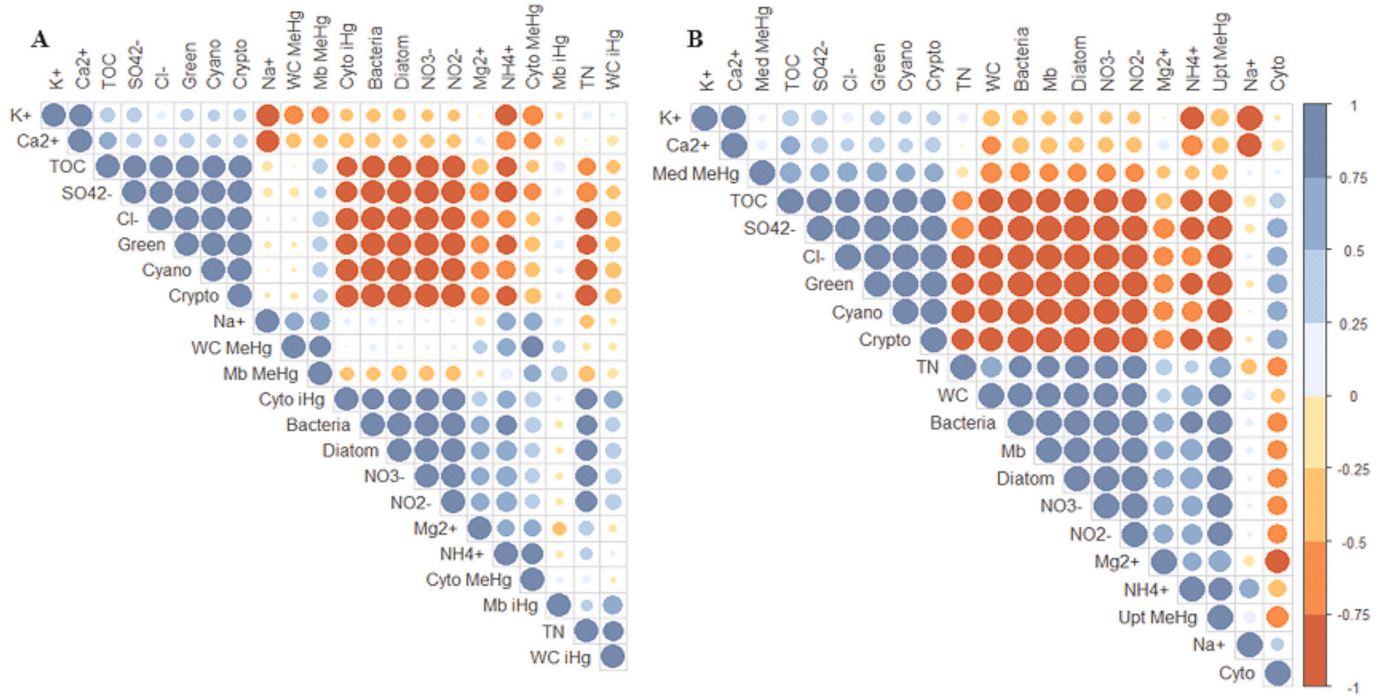

Fig. 3. Pearson correlation matrices for (A) Hg uptake and (B) MMHg biotic demethylation by pico-nanoplankton and selected physicochemical parameters of lake water and abundance of different groups determined in pico-nanoplankton. iHg: ^{199}iHg, MMHg: ^{201}MMHg, WC: whole cell, Cyto: cytosol, Mb, membrane/organelles fraction, Med: dissolved fraction in medium, Green: green algae, Cyano: cyanobacteria, Crypto: cryptophyta, Bacteria: bacterioplankton + mycoplankton, Upt: uptake. (For interpretation of the references to colour in this figure legend, the reader is referred to the Web version of this article.)

bioavailability is dependent on the complexation by DOM, competition with major ions and nature of the microorganisms (Beauvais-Fluck et al., 2019; Branfireun et al., 2020; Hsu-Kim et al., 2013).

The accumulation of iHg and MMHg in whole cells was positively correlated with the percentage of diatoms and heterotrophic microorganism present in the pico-nanoplankton and negatively correlated with the percentage of green alga, cyanobacteria and cryptophyta (Fig. 3A). These findings were consistent with a published study showing that diatoms are the major Hg accumulators in river (Tien, 2004). However, the comparison is difficult given the possible differences in community composition. Similarly, the accumulation of ^{199}iHg in both cellular compartments was positively correlated with the percentage of diatoms and heterotrophic microorganisms, as it was the case for ^{201}MMHg in the cytosol. The RDA confirmed the strong dependency of iHg and MMHg accumulation on the abundance of diatoms and heterotrophic organisms in pico-nanoplankton (Fig. S6). Overall, these results suggest that bioaccumulation and subcellular distribution of both iHg and MMHg in the natural pico-nanoplankton from eutrophic lake Soppen were dependent on both community composition and the concentrations of DOC, major cation and anion concentrations.

3.4. Biotic transformations of ^{199}iHg and ^{201}MMHg by pico-nanoplankton

The percentage of newly formed ^{201}iHg, used as a measure for ^{201}MMHg demethylation by the phyto- and bacterioplankton with a size between 0.2 and 20 μm, corresponded to 9.1 ± 1.1% and 11.8 ± 0.4% for depths 1 and 2, respectively (Fig. 4). Comparison of the proportion of ^{201}MMHg demethylated in the whole system, medium and whole cell showed that 82% of the demethylation was biologically mediated by pico-nanoplankton (Fig. S7). Biotic transformation of MMHg to iHg by aerobic and anaerobic microorganisms is considered as a major mechanism of MMHg degradation and involves reductive and oxidative demethylation (Du et al., 2019). MMHg can be also transformed abiotically by photoreduction and photodemethylation in the presence of

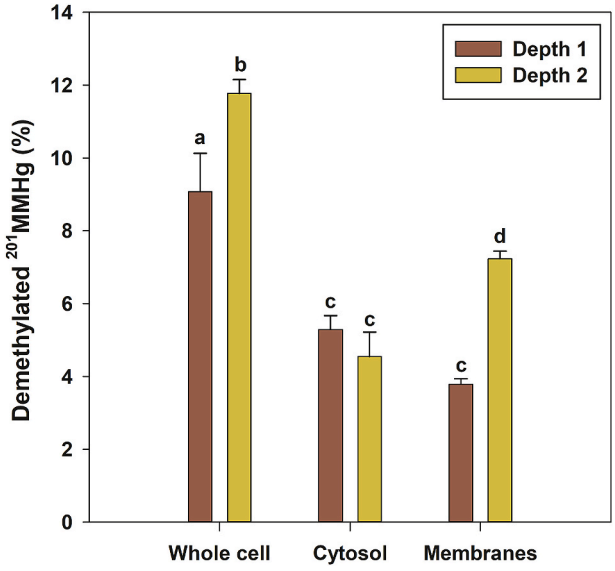

Fig. 4. Percentages of demethylated ^{201}MMHg by natural pico-nanoplankton communities exposed to an isotopic mixture of 1×10^{-9} mol L^{-1} ^{199}iHg and 0.1×10^{-9} mol L^{-1} ^{201}MMHg. Standard deviations are given for triplicate experiments (n = 3). Letters indicate statistically significant difference (Student-Newman-Keuls test with p-value < 0.05).

DOM (Jeremiason et al., 2015). However, in the eutrophic lakes characterized by higher biomass, as well as a higher turbidity Hg photoreduction/demethylation is expected to be of rather limited contribution.

The percentage of newly formed ^{201}iHg in the cytosol fraction was comparable for both pico-nanoplankton sampled at both depths. However, twice more newly formed ^{201}iHg was found in in membrane/

organelles fraction for the pico-nanoplankton from depth 2 (Fig. 4). These observations could be explained by differences in the community composition between the sampling depths (i.e. the higher abundance of diatoms and heterotrophic microorganisms at depth 2). Indeed, heterotrophic bacteria exhibit a dedicated detoxification pathway of reductive or oxidative demethylation (Gregoire and Poulain, 2014; Hsu-Kim et al., 2013). The oxidative demethylation leading to a formation of iHg, is mainly conducted by sulphate reducers and methanogens. The reductive process might occur through two pathways, one involving the *mer* operon, considered as more common and other, leading to the formation of Hg^0 and a net loss of mercury via volatilization (Grégoire et al., 2018). The obtained results are also consistent with literature pointing out that MMHg demethylation could occur in laboratory experiment with axenic culture of the green alga *C. reinhardtii* (Bravo et al., 2014). Moreover, it has been also shown that some microscopic fungi found in contaminated environments could accumulate iHg and transform it in a volatile form (Urík et al., 2014).

No significant methylation of ^{199}iHg was observed during the 24 h exposure for both communities of the lake Soppen (Fig. S8). The percentage of ^{199}MMHg formed by the transformation of ^{199}iHg by pico-nanoplankton was low, although measurable in the two subcellular fractions. It corresponded to a formation yield for ^{199}MMHg below 0.42%, a value comparable to the detection limit. These findings are consistent with the existing literature demonstrating lack of iHg methylation by different model phytoplankton (Bravo et al., 2014; Franco et al., 2018; Kelly et al., 2007; Lefebvre et al., 2007). Indeed no methylation was found for *C. reinhardtii* (exposed to 4.2×10^{-9} mol L^{-1} of $HgCl_2$ during 48 h (Bravo et al., 2014)), *Synechococcus leopoldiensis* (exposed to 7.4×10^{-7} mol L^{-1} of $HgCl_2$ during 100 h (Lefebvre et al., 2007)), *Nostoc poludosum* (exposed to 1.3×10^{-7} mol L^{-1} of $HgCl_2$ (Franco et al., 2018)), *Selenastrum minutum* or *Navicula pellicosa* (exposed to 2.2×10^{-6} mol L^{-1} of $HgCl_2$ during 48h (Kelly et al., 2007)). However, our results contrasted with previous field work showing that MMHg formation could be enhanced by the presence of cyanobacteria in floodplain of tropical regions (Lazaro et al., 2013). Other studies showed that some groups of the natural pico-nanoplankton could provide a favourable environment to methylator organisms by releasing organic molecules fuelling microbial activity (Bravo and Cosio, 2020; Heimburger et al., 2010).

The correlation matrix revealed that the percentage of demethylated ^{201}MMHg in the whole cell and membrane/organelles fraction was positively correlated with the abundance of diatoms and heterotrophic microorganisms in the pico-nanoplankton (Fig. 3B and S9). The demethylated MMHg present in cytosolic fraction was positively linked with the abundance of cyanobacteria, green algae and cryptophyta (Fig. 3B). Demethylation in whole cell and membrane/organelles fraction was positively correlated with TN, NH_4^+, Mg^{2+}, NO_3^- and NO_2^- (Fig. 3B), suggesting that demethylation may be linked with N bioavailability. Nitrogen containing enzymes are known to play a key role in electron transfers, e.g., hydroxylamine oxidoreductase, nitrite oxidase, nitrate reductase, and hydrazine dehydrogenase in different bacteria (Lin et al., 2021). A negative correlation between demethylation in the cytosol and TOC, Ca^{2+}, K^+, SO_4^{2-} and Cl^- was also found (Fig. 3B). This observation is consistent with a negative relationship between iHg and MMHg accumulated in the pico-nanoplankton cells (Fig. 3A). There are currently no studies showing if and how the demethylation process could be influenced by variation of the concentration and composition of major cations and anions.

The results of the present study demonstrated that natural pico-nanoplankton could influence Hg speciation through a demethylation, thus the role of these microorganisms is not limited to the biouptake/decrease in the ambient Hg concentration (Zhang et al., 2020). The accumulation of both Hg species and their subcellular distribution were dependent on the pico-nanoplankton community composition in the lake water column following the stratification. The subcellular distribution of iHg and MMHg in the cells has important implication for mercury trophic transfer and biomagnification in lake ecosystem, since (i) the pico-nanoplankton are at the base of the pelagic food web, and (ii) the assimilation of a pollutant is dependent on its subcellular distribution with a higher assimilation efficiency of the metals in the cytosolic fraction (Le Faucheur et al., 2014). Heterotrophic bacteria were shown to exert a differential role in Hg cycling where phytoplankton co-exist (Bravo and Cosio, 2020; Mangal et al., 2019). Further in-depth investigation of the interconnection between heterotrophic and autotrophic microorganisms will be necessary to decipher their relative importance and role in Hg biogeochemical cycle.

In the present study we have employed double-double species-specific isotope dilution analysis to follow the bioaccumulation and potential transformation of iHg and MMHg by natural pico-nanoplankton communities. Among several mathematical approaches used to study the speciation using enriched isotopes (Björn et al., 2007; Hintelmann and Evans, 1997; Lambertsson et al., 2001; Rodríguez-González et al., 2007), double-double species-specific isotope dilution analysis based on IPD brings the possibility to explore multiple biogeochemical processes in complex aquatic environments (Bouchet et al., 2018; Rodriguez-Gonzalez et al., 2013). This approach has an advantage of simultaneous and quantitative determination of newly formed and remaining species of exogenous (enriched isotopes) Hg species, but also, the quantification of endogenous (natural) iHg and MMHg (Bridou et al., 2011; Rodriguez-Gonzalez et al., 2013). The potential Hg transformations could be influenced by the medium biogeochemistry, duration of the incubation experiment, ratio between exogenous iHg and MMHg and endogenous Hg species concentrations (Bouchet et al., 2013; Bridou et al., 2011; Zhang et al., 2021). In our work, the mathematical approach based on the IPD allows correcting possible isotope exchanges reactions between endogenous and exogenous Hg species. In addition, the ratio between exogenous iHg and MMHg and exogenous and endogenous was high (26 for iHg and 17 for MMHg), thus the isotopic signature of the exogeneous Hg species is overwhelming the one of endogenous species. However, the convergence of the spiked exogenous mercury isotopes towards endogenous Hg behaviour is considered as a prerequisite for the obtaining unbiased and environmentally relevant information (Bouchet et al., 2013; Zhang et al., 2021). Further work should be therefore undertaken to compare the reaction rates of Hg chemical transformation, but also the chemical flux across biological membrane between endogenous and exogenous Hg.

4. Conclusions

The present study examined the bioaccumulation and methylation/demethylation of iHg and MMHg by natural pico-nanoplankton sampled at 2 depths in an eutrophic lake Soppen. Natural pico-nanoplankton, containing cyanobacteria, diatoms, cryptophyta, green algae and heterotrophic microorganisms, accumulated both iHg and MMHg. The whole cell concentration of ^{199}iHg was comparable in the assemblages originating from both sampling depths, however ^{201}MMHg concentration in the pico-nanoplankton in deeper samples was significantly higher. Both Hg species were predominantly accumulated in membrane/organelles and the ratios of membrane/cytosol Hg concentrations were comparable. Pico-nanoplankton communities from two depths demethylated MMHg in the cytosol and membrane/organelles, however the governing mechanisms are to be further explored. Correlation matrices built on the base of Pearson correlation coefficients revealed that iHg and MMHg uptake, and MMHg demethylation were positively correlated with the proportion of diatoms and heterotrophic microorganisms in the pico-nanoplankton, the concentrations of TN, Mg^{2+}, NO_3^-, NO_2^-, NH_4^+ and negatively correlated with the concentrations of DOC, K^+, Na^+, Ca^{2+}; SO_4^{2-}. No significant methylation of iHg by pico-nanoplankton was found during the 24 h exposure. Overall, this study provides a novel and an original information about the role of pico- and nanoplankton in Hg biogeochemical cycle, however further study needs to be done to understand the interconnection between heterotrophic and

autotrophic microorganisms.

Author statement

TC and VIS proposed the concept. TC, JG, ET, DA and VIS have developed the experimental design. TC and KK participated to water sampling, CTD and fluoroprobe profiles. KK characterized chemistry parameters of lake water. TC realized mercury exposure of pico-nanoplankton communities and all data treatment.. JG, ET, ZP and DA have established the isotopic tracer's incubation conceptual framework and methodology, performed sample preparation and measurement compound specific isotopic dilution measurements and data processing. TC, IW and VIS provided interpretation of data. VIS overviewed the study. All authors have participated in the manuscript writing. All the authors have approved the paper submission. In the name of the authors, I attest that the enclosed manuscript has not been previously in whole or in part and is not under consideration by any journal. I also affirm that the authors are aware of and accept responsibility for the manuscript.

Declaration of competing interest

The authors declare that they have no known competing financial interests or personal relationships that could have appeared to influence the work reported in this paper.

Acknowledgement

This work was supported by the Swiss National Science Foundation (SNSF, project No 175721) and the French "Agence Nationale de la Recherche" (ANR, project No17-CE34-0014-01). Warm thanks are extended to Dan McGinnins and his team for the help with field sampling and in-situ measurement with a special thanks for Timon Langenegger. Authors acknowledge Pierre Marle for his help with statistical analysis.

Appendix A. Supplementary data

Supplementary data to this article can be found online at https://doi.org/10.1016/j.envpol.2021.117771.

References

Beauvais-Fluck, R., Slaveykova, V.I., Cosio, C., 2017. Cellular toxicity pathways of inorganic and methyl mercury in the green microalga Chlamydomonas reinhardtii. Sci. Rep. 7, 8034.

Beauvais-Fluck, R., Slaveykova, V.I., Ulf, S., Cosio, C., 2019. Towards early-warning gene signature of Chlamydomonas reinhardtii exposed to Hg-containing complex media. Aquat. Toxicol. 214, 105259.

Björn, E., Larsson, T., Lambertsson, L., Skyllberg, U., Frech, W., 2007. Recent advances in mercury speciation analysis with focus on spectrometric methods and enriched stable isotope applications. Ambio 36, 443–451.

Bouchet, S., Goni-Urriza, M., Monperrus, M., Guyoneaud, R., Fernandez, P., Heredia, C., Tessier, E., Gassie, C., Point, D., Guedron, S., Acha, D., Amouroux, D., 2018. Linking microbial activities and low-molecular-weight thiols to Hg methylation in biofilms and periphyton from high-altitude tropical lakes in the Bolivian altiplano. Environ. Sci. Technol. 52, 9758–9767.

Bouchet, S., Rodriguez-Gonzalez, P., Bridou, R., Monperrus, M., Tessier, E., Anschutz, P., Guyoneaud, R., Amouroux, D., 2013. Investigations into the differential reactivity of endogenous and exogenous mercury species in coastal sediments. Environ. Sci. Pollut. Res. Int. 20, 1292–1301.

Boullemant, A., Lavoie, M., Fortin, C., Campbell, P.G.C., 2009. Uptake of hydrophobic metal complexes by three freshwater algae: unexpected influence of pH. Environ. Sci. Technol. 43, 3308–3314.

Branfireun, B.A., Cosio, C., Poulain, A.J., Riise, G., Bravo, A.G., 2020. Mercury cycling in freshwater systems - an updated conceptual model. Sci. Total Environ. 745.

Bratkic, A., Tinta, T., Koron, N., Guevara, S.R., Begu, E., Barkay, T., Horvat, M., Falnoga, I., Faganeli, J., 2018. Mercury transformations in a coastal water column (Gulf of Trieste, northern Adriatic Sea). Mar. Chem. 200, 57–67.

Bravo, A.G., Bouchet, S., Tolu, J., Bjorn, E., Mateos-Rivera, A., Bertilsson, S., 2017. Molecular composition of organic matter controls methylmercury formation in boreal lakes. Nat. Commun. 8, 14255.

Bravo, A.G., Cosio, C., 2020. Biotic formation of methylmercury: a bio-physico-chemical conundrum. Limnol. Oceanogr. 65, 1010–1027.

Bravo, A.G., Le Faucheur, S., Monperrus, M., Amouroux, D., Slaveykova, V.I., 2014. Species-specific isotope tracers to study the accumulation and biotransformation of mixtures of inorganic and methyl mercury by the microalga Chlamydomonas reinhardtii. Environ. Pollut. 192, 212–215.

Bridou, R., Monperrus, M., Gonzalez, P.R., Guyoneaud, R., Amouroux, D., 2011. Simultaneous determination of mercury methylation and demethylation capacities of various sulfate-reducing bacteria using species-specific isotopic tracers. Environ. Toxicol. Chem. 30, 337–344.

Chen, C.Y., Pickhardt, P.C., Xu, M.Q., Folt, C.L., 2008. Mercury and arsenic bioaccumulation and eutrophication in Baiyangdian Lake, China. Water Air Soil Pollut. 190, 115–127.

Chen, H.W., Wu, Y.Y., Li, Y.X., Huang, W.J., 2014. Methylmercury accumulation and toxicity to cyanobacteria: implications of extracellural polymeric substances and growth properties. Water Environ. Res. 86, 626–634.

Chen, L., Zhang, X., Cao, M., Pan, Y., Xiao, C., Wang, P., Liang, Y., Liu, G., Cai, Y., 2021. Release of legacy mercury and effect of aquaculture on mercury biogeochemical cycling in highly polluted Ya-Er Lake, China. Chemosphere 275, 130011.

Coclet, C., Garnier, C., Durrieu, G., Omanović, D., D'Onofrio, S., Le Poupon, C., Mullot, J.-U., Briand, J.-F., Misson, B., 2019. Changes in bacterioplankton communities resulting from direct and indirect interactions with trace metal gradients in an urbanized marine coastal area. Front. Microbiol. 10.

Crist, T.O., Veech, J.A., Gering, J.C., Summerville, K.S., 2003. Partitioning species diversity across landscapes and regions: a hierarchical analysis of alpha, beta, and gamma diversity. Am. Nat. 162, 734–743.

Delpy, F., Serranito, B., Jamet, J.L., Gregori, G., Le Poupon, C., Jamet, D., 2018. Pico- and nanophytoplankton dynamics in two coupled but contrasting coastal bays in the NW mediterranean sea (France). Estuar. Coast 41, 2039–2055.

Deng, L., Fu, D., Deng, N., 2009. Photo-induced transformations of mercury(II) species in the presence of algae, Chlorella vulgaris. J. Hazard Mater. 164, 798–805.

Deng, L., Wu, F., Deng, N., Zuo, Y., 2008. Photoreduction of mercury(II) in the presence of algae, Anabaena cylindrical. J. Photochem. Photobiol. B Biol. 91, 117–124.

Dranguet, P., Cosio, C., Le Faucheur, S., Beauvais-Fluck, R., Freiburghaus, A., Worms, I. A.M., Petit, B., Civic, N., Docquier, M., Slaveykova, V.I., 2017. Transcriptomic approach for assessment of the impact on microalga and macrophyte of in-situ exposure in river sites contaminated by chlor-alkali plant effluents. Water Res. 121, 86–94.

Dranguet, P., Fluck, R., Regier, N., Cosio, C., Le Faucheur, S., Slaveykova, V.I., 2014. Towards mechanistic understanding of mercury availability and toxicity to aquatic primary producers. Chimia 68, 799–805.

Driscoll, C.T., Chen, C.Y., Hammerschmidt, C.R., Mason, R.P., Gilmour, C.C., Sunderland, E.M., Greenfield, B.K., Buckman, K.L., Lamborg, C.H., 2012. Nutrient supply and mercury dynamics in marine ecosystems: a conceptual model. Environ. Res. 119, 118–131.

Driscoll, C.T., Mason, R.P., Chan, H.M., Jacob, D.J., Pirrone, N., 2013. Mercury as a global pollutant: sources, pathways, and effects. Environ. Sci. Technol. 47, 4967–4983.

Du, H.X., Ma, M., Igarashi, Y., Wang, D.Y., 2019. Biotic and abiotic degradation of methylmercury in aquatic ecosystems: a review. Bull. Environ. Contam. Toxicol. 102, 605–611.

Eagles-Smith, C.A., Wiener, J.G., Eckley, C.S., Willacker, J.J., Evers, D.C., Marvin-DiPasquale, M., Obrist, D., Fleck, J.A., Aiken, G.R., Lepak, J.M., Jackson, A.K., Webster, J.P., Stewart, A.R., Davis, J.A., Alpers, C.N., Ackerman, J.T., 2016. Mercury in western North America: a synthesis of environmental contamination, fluxes, bioaccumulation, and risk to fish and wildlife. Sci. Total Environ. 568, 1213–1226.

Ellwood, M.J., Hunter, K.A., 2000. The incorporation of zinc and iron into the frustule of the marine diatom Thalassiosira pseudonana. Limnol. Oceanogr. 45, 1517–1524.

Franco, M.W., Mendes, L.A., Windmoller, C.C., Moura, K.A.F., Oliveira, L.A.G., Barbosa, F.A.R., 2018. Mercury methylation capacity and removal of Hg species from aqueous medium by cyanobacteria. Water Air Soil Pollut. 229, 127.

French, T.D., Houben, A.J., Desforges, J.-P.W., Kimpe, L.E., Kokelj, S.V., Poulain, A.J., Smol, J.P., Wang, X., Blais, J.M., 2014. Dissolved organic carbon thresholds affect mercury bioaccumulation in arctic lakes. Environ. Sci. Technol. 48, 3162–3168.

Friendly, M., 2002. Corrgrams: exploratory displays for correlation matrices. Am. Statistician 56, 316–324.

Garrido, M., Cecchi, P., Malet, N., Bec, B., Torre, F., Pasqualini, V., 2019. Evaluation of FluoroProbe® performance for the phytoplankton-based assessment of the ecological status of Mediterranean coastal lagoons. Environ. Monit. Assess. 191, 204.

Gregoire, D.S., Poulain, A.J., 2014. A little bit of light goes a long way: the role of phototrophs on mercury cycling. Metall 6, 396–407.

Grégoire, D.S., Poulain, A.J., Ivanova, E.P., 2018. Shining light on recent advances in microbial mercury cycling. FACETS 3, 858–879.

Gruber, N., Wehrli, B., Wuest, A., 2000. The role of biogeochemical cycling for the formation and preservation of varved sediments in Soppensee (Switzerland). J. Paleolimnol. 24, 277–291.

Gu, B., Mishra, B., Miller, C., Wang, W., Lai, B., Brooks, S.C., Kemner, K.M., Liang, L., 2014. X-ray fluorescence mapping of mercury on suspended mineral particles and diatoms in a contaminated freshwater system. Biogeosciences 11, 5259–5267.

Guédron, S., Point, D., Acha, D., Bouchet, S., Baya, P.A., Tessier, E., Monperrus, M., Molina, C.I., Groleau, A., Chauvaud, L., Thebault, J., Amice, E., Alanoca, L., Duwig, C., Uzu, G., Lazzaro, X., Bertrand, A., Bertrand, S., Barbraud, C., Delord, K., Gibon, F.M., Ibanez, C., Flores, M., Fernandez Saavedra, P., Ezpinoza, M.E., Heredia, C., Rocha, F., Zepita, C., Amouroux, D., 2017. Mercury contamination level and speciation inventory in Lakes Titicaca & Uru-Uru (Bolivia): current status and future trends. Environ. Pollut. 231, 262–270.

Hamilton, D.P., O'Brien, K.R., Burford, M.A., Brookes, J.D., McBride, C.G., 2010. Vertical distributions of chlorophyll in deep, warm monomictic lakes. Aquat. Sci. 72, 295–307.
Heimburger, L.E., Cossa, D., Marty, J.C., Migon, C., Averty, B., Dufour, A., Ras, J., 2010. Methyl mercury distributions in relation to the presence of nano- and picophytoplankton in an oceanic water column (Ligurian Sea, North-western Mediterranean). Geochem. Cosmochim. Acta 74, 5549–5559.
Herrero Ortega, S., Catalán, N., Björn, E., Gröntoft, H., Hilmarsson, T.G., Bertilsson, S., Wu, P., Bishop, K., Levanoni, O., Bravo, A.G., 2018. High methylmercury formation in ponds fueled by fresh humic and algal derived organic matter. Limnol. Oceanogr. 63, S44–S53.
Hintelmann, H., Evans, R.D., 1997. Application of stable isotopes in environmental tracer studies – measurement of monomethylmercury (CH3Hg+) by isotope dilution ICP-MS and detection of species transformation. Fresen. J. Anal. Chem. 358, 378–385.
Hsu-Kim, H., Kucharzyk, K.H., Zhang, T., Deshusses, M.A., 2013. Mechanisms regulating mercury bioavailability for methylating microorganisms in the aquatic environment: a critical review. Environ. Sci. Technol. 47, 2441–2456.
Husson, F., Josse, J., Lê, S., 2008. FactoMineR: an R package for multivariate analysis. J. Stat. Software 25, 1–18.
Jaccard, T., Ariztegui, D., Wilkinson, K.J., 2009. Incorporation of zinc into the frustule of the freshwater diatom Stephanodiscus hantzschii. Chem. Geol. 265, 381–386.
Jeremiason, J.D., Portner, J.C., Aiken, G.R., Hiranaka, A.J., Dvorak, M.T., Tran, K.T., Latch, D.E., 2015. Photoreduction of Hg(ii) and photodemethylation of methylmercury: the key role of thiol sites on dissolved organic matter. Environ Sci Process Impacts 17, 1892–1903.
Kelly, C.A., Rudd, J.W.M., Holoka, M.H., 2003. Effect of pH on mercury uptake by an aquatic bacterium: implications for Hg cycling. Environ. Sci. Technol. 37, 2941–2946.
Kelly, D., Budd, K., Lefebvre, D.D., 2006. Mercury analysis of acid- and alkaline-reduced biological samples: identification of meta-cinnabar as the major biotransformed compound in algae. Appl. Environ. Microbiol. 72, 361–367.
Kelly, D.J.A., Budd, K., Lefebvre, D.D., 2007. Biotransformation of mercury in pH-stat cultures of eukaryotic freshwater algae. Arch. Microbiol. 187, 45–53.
Kim, H., Van Duong, H., Kim, E., Lee, B.G., Han, S., 2014. Effects of phytoplankton cell size and chloride concentration on the bioaccumulation of methylmercury in marine phytoplankton. Environ. Toxicol. 29, 936–941.
Kritee, K., Motta, L.C., Blum, J.D., Tsui, M.T.K., Reinfelder, J.R., 2018. Photomicrobial visible light-induced magnetic mass independent fractionation of mercury in a marine microalga. Acs Earth and Space Chemistry 2, 432–440.
Lambertsson, L., Lundberg, E., Nilsson, M., Frech, W., 2001. Applications of enriched stable isotope tracers in combination with isotope dilution GC-ICP-MS to study mercury species transformation in sea sediments during in situ ethylation and determination. J. Anal. At. Spectrom. 16, 1296–1301.
Langenegger, T., Vachon, D., Donis, D., McGinnis, D.F., 2019. What the bubble knows: lake methane dynamics revealed by sediment gas bubble composition. Limnol. Oceanogr. 64, 1526–1544.
Lanza, W.G., Acha, D., Point, D., Masbou, J., Alanoca, L., Amouroux, D., Lazzaro, X., 2017. Association of a specific algal group with methylmercury accumulation in periphyton of a tropical high-altitude andean lake. Arch. Environ. Contam. Toxicol. 72, 1–10.
Lavoie, R.A., Amyot, M., Lapierre, J.F., 2019. Global meta-analysis on the relationship between mercury and dissolved organic carbon in freshwater environments. Journal of Geophysical Research-Biogeosciences 124, 1508–1523.
Lazaro, W.L., Guimaraes, J.R.D., Ignacio, A.R.A., Da Silva, C.J., Diez, S., 2013. Cyanobacteria enhance methylmercury production: a hypothesis tested in the periphyton of two lakes in the Pantanal floodplain, Brazil. Sci. Total Environ. 456, 231–238.
Le Faucheur, S., Campbell, P.G.C., Fortin, C., Slaveykova, V.I., 2014. Interactions between mercury and phytoplankton: speciation, bioavailability, and internal handling. Environ. Toxicol. Chem. 33, 1211–1224.
Le Faucheur, S., Tremblay, Y., Fortin, C., Campbell, P.G.C., 2011. Acidification increases mercury uptake by a freshwater alga, Chlamydomonas reinhardtii. Environ. Chem. 8, 612–622.
Leach, T.H., Beisner, B.E., Carey, C.C., Pernica, P., Rose, K.C., Huot, Y., Brentrup, J.A., Domaizon, I., Grossart, H.P., Ibelings, B.W., Jacquet, S., Kelly, P.T., Rusak, J.A., Stockwell, J.D., Straile, D., Verburg, P., 2018. Patterns and drivers of deep chlorophyll maxima structure in 100 lakes: the relative importance of light and thermal stratification. Limnol. Oceanogr. 63, 628–646.
Lee, C.S., Fisher, N.S., 2016. Methylmercury uptake by diverse marine phytoplankton. Limnol. Oceanogr. 61, 1626–1639.
Lee, C.S., Fisher, N.S., 2017. Bioaccumulation of methylmercury in a marine diatom and the influence of dissolved organic matter. Mar. Chem. 197, 70–79.
Lefebvre, D.D., Kelly, D., Budd, K., 2007. Biotransformation of Hg(II) by cyanobacteria. Appl. Environ. Microbiol. 73, 243–249.
Lin, C.C., Yee, N., Barkay, T., 2011. Microbial Transformations in the Mercury Cycle, Environmental Chemistry and Toxicology of Mercury. G. Liu, Y. Cai and N. O'Driscoll, pp. 155–191.
Lin, H., Ascher, D.B., Myung, Y., Lamborg, C.H., Hallam, S.J., Gionfriddo, C.M., Holt, K. E., Moreau, J.W., 2021. Mercury methylation by metabolically versatile and cosmopolitan marine bacteria. ISME J.
Lotter, A.F., 2001. The palaeolimnology of Soppensee (Central Switzerland), as evidenced by diatom, pollen, and fossil-pigment analyses. J. Paleolimnol. 25, 65–79.
Mangal, V., Stenzler, B.R., Poulain, A.J., Gueguen, C., 2019. Aerobic and anaerobic bacterial mercury uptake is driven by algal organic matter composition and molecular weight. Environ. Sci. Technol. 53, 157–165.
Monperrus, M., Gonzalez, P.R., Amouroux, D., Alonso, J.I.G., Donard, O.F.X., 2008. Evaluating the potential and limitations of double-spiking species-specific isotope dilution analysis for the accurate quantification of mercury species in different environmental matrices. Anal. Bioanal. Chem. 390, 655–666.
Monperrus, M., Tessier, E., Amouroux, D., Leynaert, A., Huonnic, P., Donard, O.F.X., 2007. Mercury methylation, demethylation and reduction rates in coastal and marine surface waters of the Mediterranean Sea. Mar. Chem. 107, 49–63.
Mu, W.J., Jia, K., Liu, Y., Pan, X.M., Fan, Y.W., 2017. Response of the freshwater diatom Halamphora veneta (Kutzing) Levkov to copper and mercury and its potential for bioassessment of heavy metal toxicity in aquatic habitats. Environ. Sci. Pollut. Control Ser. 24, 26375–26386.
Pedrero, Z., Bridou, R., Mounicou, S., Guyoneaud, R., Monperrus, M., Amouroux, D., 2012. Transformation, localization, and biomolecular binding of Hg species at subcellular level in methylating and nonmethylating sulfate-reducing bacteria. Environ. Sci. Technol. 46, 11744–11751.
Pickhardt, P.C., Fisher, N.S., 2007. Accumulation of inorganic and methylmercury by freshwater phytoplankton in two contrasting water bodies. Environ. Sci. Technol. 41, 125–131.
Poste, A.E., Muir, D.C.G., Guildford, S.J., Hecky, R.E., 2015. Bioaccumulation and biomagnification of mercury in African lakes: the importance of trophic status. Sci. Total Environ. 506, 126–136.
Razavi, N.R., Qu, M., Chen, D., Zhong, Y., Ren, W., Wang, Y., Campbell, L.M., 2015. Effect of eutrophication on mercury (Hg) dynamics in subtropical reservoirs from a high Hg deposition ecoregion. Limnol. Oceanogr. 60, 386–401.
Rodriguez-Gonzalez, P., Bouchet, S., Monperrus, M., Tessier, E., Amouroux, D., 2013. In situ experiments for element species-specific environmental reactivity of tin and mercury compounds using isotopic tracers and multiple linear regression. Environ. Sci. Pollut. Control Ser. 20, 1269–1280.
Rodríguez-González, P., Monperrus, M., García Alonso, J.I., Amouroux, D., Donard, O.F. X., 2007. Comparison of different numerical approaches for multiple spiking species-specific isotope dilution analysis exemplified by the determination of butyltin species in sediments. J. Anal. At. Spectrom. 22, 1373–1382.
Schutte, C.A., Samarkin, V.A., Peters, B., Madigan, M.T., Bowles, M., Morgan-Kiss, R., Casciotti, K., Joye, S., 2020. Vertical stratification and stability of biogeochemical processes in the deep saline waters of Lake Vanda, Antarctica. Limnol. Oceanogr. 65, 569–581.
Sieburth, J.M., Smetacek, V., Lenz, J., 1978. Pelagic ecosystem structure - heterotrophic compartments of plankton and their relationship to plankton size fractions. Limnol. Oceanogr. 23, 1256–1263.
Sigel, A., Sigel, H., Sigel, R.K.O., 2015. Organometallics in Environment and Toxicology. Walter de Gruyter GmbH & Co KG.
Simmonds, B., Wood, S.A., Ozkundakci, D., Hamilton, D.P., 2015. Phytoplankton succession and the formation of a deep chlorophyll maximum in a hypertrophic volcanic lake. Hydrobiologia 745, 297–312.
Skrobonja, A., Gojkovic, Z., Soerensen, A.L., Westlund, P.O., Funk, C., Bjorn, E., 2019. Uptake kinetics of methylmercury in a freshwater alga exposed to methylmercury complexes with environmentally relevant thiols. Environ. Sci. Technol. 53, 13757–13766.
Soerensen, A.L., Schartup, A.T., Gustafsson, E., Gustafsson, B.G., Undeman, E., Björn, E., 2016. Eutrophication increases phytoplankton methylmercury concentrations in a coastal sea—a baltic sea case study. Environ. Sci. Technol. 50, 11787–11796.
Streets, D.G., Horowitz, H.M., Jacob, D.J., Lu, Z., Levin, L., ter Schure, A.F.H., Sunderland, E.M., 2017. Total mercury released to the environment by human activities. Environ. Sci. Technol. 51, 5969–5977.
Tang, K.W., Flury, S., Vachon, D., Ordonez, C., McGinnis, D.F., 2018. The phantom midge menace: migratory Chaoborus larvae maintain poor ecosystem state in eutrophic inland waters. Water Res. 139, 30–37.
Tien, C.J., 2004. Some aspects of water quality in a polluted lowland river in relation to the intracellular chemical levels in planktonic and epilithic diatoms. Water Res. 38, 1779–1790.
Urík, M., Hlodák, M., Mikušová, P., Matúš, P., 2014. Potential of microscopic fungi isolated from mercury contaminated soils to accumulate and volatilize mercury(II). Water, air. & Soil Pollution 225, 2219.
Vachon, D., Langenegger, T., Donis, D., McGinnis, D.F., 2019. Influence of water column stratification and mixing patterns on the fate of methane produced in deep sediments of a small eutrophic lake. Limnol. Oceanogr. 64, 2114–2128.
Van, L.N., Jonsson, S., Skyllberg, U., Nilsson, M.B., Andersson, A., Lundberg, E., Bjorn, E., 2016. Effects of nutrient loading and mercury chemical speciation on the formation and degradation of methylmercury in estuarine sediment. Environ. Sci. Technol. 50, 6983–6990.
Wang, F., Lemes, M., Khan, M.A.K., 2011. Metallomics of Mercury: Role of Thiol- and Selenol-Containing Biomolecules, Environmental Chemistry and Toxicology of Mercury. John Wiley & Sons, Ltd, pp. 517–544.
Wang, M.Z., Xu, X.W., Wu, Z., Zhang, X.Q., Sun, P.Z., Wen, Y.T., Wang, Z., Lu, X.B., Zhang, W., Wang, X.J., Tong, Y.D., 2019. Seasonal pattern of nutrient limitation in a eutrophic lake and quantitative analysis of the impacts from internal nutrient cycling. Environ. Sci. Technol. 53, 13675–13686.
Wang, S., Xing, D., Jia, Y., Li, B., Wang, K., 2012a. The distribution of total mercury and methyl mercury in a shallow hypereutrophic lake (Lake Taihu) in two seasons. Appl. Geochem. 27, 343–351.
Wang, S., Zhang, M., Li, B., Xing, D., Wang, X., Wei, C., Jia, Y., 2012b. Comparison of mercury speciation and distribution in the water column and sediments between the algal type zone and the macrophytic type zone in a hypereutrophic lake (Dianchi Lake) in Southwestern China. Sci. Total Environ. 417–418, 204–213.

Wang, S.F., Li, B., Zhang, M.M., Xing, D.H., Jia, Y.F., Wei, C.Y., 2012c. Bioaccumulation and trophic transfer of mercury in a food web from a large, shallow, hypereutrophic lake (Lake Taihu) in China. Environ. Sci. Pollut. Control Ser. 19, 2820–2831.
Wetzel, R.G., 2001. Limnology: Lake and River Ecosystems. Gulf Professional Publishing.
Wu, P.P., Zakem, E.J., Dutkiewicz, S., Zhang, Y.X., 2020. Biomagnification of methylmercury in a marine plankton ecosystem. Environ. Sci. Technol. 54, 5446–5455.
Wu, Y., Wang, W.-X., 2014. Intracellular speciation and transformation of inorganic mercury in marine phytoplankton. Aquat. Toxicol. 148, 122–129.
Wu, Y., Wang, W.X., 2011. Accumulation, subcellular distribution and toxicity of inorganic mercury and methylmercury in marine phytoplankton. Environ. Pollut. 159, 3097–3105.
Wu, Y., Wang, W.X., 2013. Differential acclimation of a marine diatom to inorganic mercury and methylmercury exposure. Aquat. Toxicol. 138, 52–59.
Yang, L., Zhang, W., Ren, M., Cao, F., Chen, F., Zhang, Y., Shang, L., 2020. Mercury distribution in a typical shallow lake in northern China and its re-emission from sediment. Ecotoxicol. Environ. Saf. 192, 110316.
Yu, C.X., Li, Z.Y., Xu, Z.H., Yang, Z.F., 2020. Lake recovery from eutrophication: quantitative response of trophic states to anthropogenic influences. Ecol. Eng. 143.
Zhang, L., Liang, X., Wang, Q., Zhang, Y., Yin, X., Lu, X., Pierce, E.M., Gu, B., 2021. Isotope exchange between mercuric [Hg(II)] chloride and Hg(II) bound to minerals and thiolate ligands: implications for enriched isotope tracer studies. Geochem. Cosmochim. Acta 292, 468–481.
Zhang, Y.X., Soerensen, A.L., Schartup, A.T., Sunderland, E.M., 2020. A global model for methylmercury formation and uptake at the base of marine food webs. Global Biogeochem. Cycles 34.